ELSEVIER

Chemical Engineering Journal 106 (2005) 145–152

Chemical Engineering Journal

www.elsevier.com/locate/cej

Sulphur oxides emission during fluidised-bed catalytic cracking

R. Maya-Yescas[a,*], E.F. Villafuerte-Macías[b,c], R. Aguilar[b], D. Salazar-Sotelo[d]

[a] *Facultad de Ingeniería Química, Universidad Michoacana de San Nicolás de Hidalgo, Ciudad Universitaria, 58190 Morelia, Michoacán, México*
[b] *Departamento de Energía, Universidad Autónoma Metropolitana – Azc, México*
[c] *Departamento de Ciencia Básica, ESIQIE, Instituto Politécnico Nacional, México*
[d] *Profesor-investigador. Universidad La Salle, Escuela de Ciencias Químicas, México*

Received 9 November 2003; received in revised form 29 September 2004; accepted 19 November 2004

Abstract

Fluidised-bed catalytic cracking (FCC) of heavy gas oils into high value liquid fuels is a common practice in the oil refining industry. In this process pollutant compounds, such as sulphur in feedstock, are redistributed into products and emissions. In this work, sulphur balance is performed around an industrial FCC unit considering riser and regenerator as coupled reactors. This issue is accomplished by considering formation of sulphur oxides during catalyst regeneration. Also, using a kinetic model that considers explicitly the formation of hydrogen sulphide during the catalytic cracking of the feedstock, an estimation of sulphur distribution in the products is performed. A mathematical model for the process is tuned using industrial data and solved to predict operating regions of the industrial unit at different conditions. Simulation results indicate the portion of sulphur in the feedstock that goes to fuels and the portion that is lost as emissions from the processes. An operating region is proposed in order to comply with requirements of low sulphur content in fuels and low level of sulphur oxides emissions.
© 2004 Elsevier B.V. All rights reserved.

Keywords: Catalytic cracking; Emissions; Fuels; Sulphur balance; Sulphur oxides

1. Introduction

During its 60-year evolution, fluidised-bed catalytic cracking (FCC) has become one of the most important oil refining processes. Currently, FCC operates in constrained regions of medium to high conversion, using synthetic catalysts. The most common FCC feedstock is a blend of gas oils, from vacuum and atmospheric distillation and/or delayed coking. This feedstock is converted into valuable fuels, such as gasoline and C_3–C_4 olefins. During the last 10 years, environmental concerns about this process have increased, because of its great contribution to the gasoline pool and, consequently, the amount of sulphur of such gasoline. Moreover, due to the internal coke combustion, this process also emits sulphur oxides (SO_x) from the catalyst regenerator.

FCC units consist of two coupled reactors (Fig. 1). The first one is a transported solid bed reactor, known as “riser”. In this unit, preheated liquid feedstock is supplied close to the bottom and dispersed with medium pressure steam. Meanwhile, hot catalyst coming from the regenerator, a fluidised bed, is supplied in order to both heat and evaporate the feedstock and to be the active surface where the catalytic cracking will take place. Both the vapour reactant mixture and the solid catalyst move upward for 2–5 s through the top of the riser, where they are separated by using a cyclone. Vapour products are directed to a fractionation tower and solid catalyst is directed to a stripper to remove adsorbed vapour hydrocarbons that are incorporated to the product stream. After stripping, catalyst moves to the regenerator where the solid by-product, known as coke, is burned-off in order to recover catalyst activity and heat necessary for feedstock evaporation and chemical reactions. Once the catalyst is regenerated, it returns to the riser and the cycle is repeated inside the unit.

Usually, FCC feed stock contains significant amounts of sulphur. Moreover, during refining of medium and heavy

---

* Corresponding author.
E-mail addresses: rafaelmayayescas@yahoo.com.mx, rmaya@zeus.umich.mx (R. Maya-Yescas), dss@ulsa.mx (D. Salazar-Sotelo).

1385-8947/$ – see front matter © 2004 Elsevier B.V. All rights reserved.
doi:10.1016/j.cej.2004.11.012

Nomenclature

a, b, c	numerical coefficients (dimensionless)
a_v	surface area of particle ($\mathrm{m^2/m^3}$)
c	concentration of lump "A" in gas phase ($\mathrm{kmol/m^3}$)
$C_\mathrm{A(P)}$	concentration of lump "A" in solid phase ($\mathrm{kmol/m^3}$)
$C^0_\mathrm{A(P)}$	initial concentration of lump "A" in solid phase ($\mathrm{kmol/m^3}$)
$C^i_{p\mathrm{AIR}}$	specific heat of gas of air (kJ/kg K)
$C_{p\mathrm{dp}}$	specific heat of gas of dense phase (kJ/kg K)
$C_{p(\mathrm{G})}$	specific heat of gas (kJ/kg K)
$C_{p\mathrm{gch}}$	specific heat of gas of dilute phase (kJ/kg K)
$C_{p\mathrm{P}}$	specific heat of catalyst particles (kJ/kg K)
$C_{p(\mathrm{P})}$	specific heat of catalyst particles (kJ/kg K)
$C_{p\mathrm{VAP}}$	specific heat of gas of steam (kJ/kg K)
d_p	particles diameter (m)
D_V	molecular diffusivity ($\mathrm{m^2/s}$)
$E_{\mathrm{feedstock}-j}$	activation energy of feedstock cracking (kJ/mol)
$E_\mathrm{lump-j}$	activation energy of lumps cracking (kJ/mol)
G_CO	CO molar flow in dilute phase (kmol/s)
$G_{\mathrm{CO_2}}$	$\mathrm{CO_2}$ molar flow in dilute phase (kmol/s)
G^i_CO	initial CO molar flow (kmol/s)
$G^i_{\mathrm{CO_2}}$	initial $\mathrm{CO_2}$ molar flow (kmol/s)
G_g	flux of gas ($\mathrm{kg/m^2\,s}$)
$G_{\mathrm{H_2O}}$	$\mathrm{H_2O}$ molar flow in dilute phase (kmol/s)
$G^i_{\mathrm{N_2}}$	$\mathrm{N_2}$ molar flow in dilute phase (kmol/s)
$G_{\mathrm{O_2}}$	$\mathrm{O_2}$ molar flow in dilute phase (kmol/s)
$G^i_{\mathrm{O_2}}$	initial $\mathrm{O_2}$ molar flow in air (kmol/s)
G_{SO_x}	SO_x molar flow in dilute phase (kmol/s)
$G^i_{\mathrm{SO}_x}$	initial SO_x molar flow (kmol/s)
$G^i_{\mathrm{N_2}}$	initial $\mathrm{N_2}$ molar flow (kmol/s)
G^i_VAP	initial steam molar flow (kmol/s)
h_g	heat transfer coefficient ($\mathrm{kJ/m^2\,s}$)
$(\Delta H)_\mathrm{HNC}$	heat of reaction of jth lump (dilute phase) (kJ/kg)
(ΔH_j)	heat of reaction of jth lump (dense phase) (kJ/kg)
$(\Delta H_\mathrm{r})_j$	heat of reaction of jth lump "(in riser) (kJ/kg)
$k_{\mathrm{feedstock}-j}$	kinetic frequency factor feedstock–lump cracking ($\mathrm{s^{-1}}$)
k_g	mass transfer coefficient (m/s)
$k_{(\mathrm{g})}$	gas thermal conductivity (W/mK)
$k_{\mathrm{lump}-j}$	kinetic frequency factor lump–lump cracking ($\mathrm{s^{-1}}$)
m_CAT	catalyst investment (kg)
m^i_CAT	initial catalyst investment (kg)
N_COdp	CO molar flow in dense phase (kmol/s)
$N_{\mathrm{CO_2dp}}$	$\mathrm{CO_2}$ molar flow in dense phase (kmol/s)
$N_{\mathrm{O_2dp}}$	$\mathrm{O_2}$ molar flow in dense phase (kmol/s)
$N_{\mathrm{SO}_x\mathrm{dp}}$	SO_x molar flow in dense phase (kmol/s)
PM_j	lump molecular weight (kg/kmol)
$R_\mathrm{CO}\vert_\mathrm{dp}$	kinetic for CO in dense phase (kmol/s)
$R_{\mathrm{CO_2}}\vert_\mathrm{dp}$	kinetic for $\mathrm{CO_2}$ in dense phase (kmol/s)
$R_\mathrm{CO}\vert_\mathrm{fb}$	kinetic for CO in dilute phase (kmol/s)
$R_{\mathrm{CO_2}}\vert_\mathrm{fb}$	kinetic for $\mathrm{CO_2}$ in dilute phase (kmol/s)
R_g	gas law constant (kJ/mol K)
$R_{\mathrm{H_2O}}\vert_\mathrm{fb}$	kinetic for $\mathrm{H_2O}$ in dilute phase (kmol/s)
R_j	reaction rate for the jth lump ($\mathrm{kmol/m^3\,s}$)
$R_{\mathrm{O_2}}\vert_\mathrm{dp}$	kinetic for $\mathrm{O_2}$ in dense phase (kmol/s)
$R_{\mathrm{SO}_x}\vert_\mathrm{dp}$	Kinetic for SO_x in dense phase (kmol/s)
$R_{\mathrm{O_2}}\vert_\mathrm{fb}$	kinetic for $\mathrm{O_2}$ in dilute phase (kmol/s)
S_LC	sulphur content in cracking products (lumps) (dimensionless)
T	temperature (K)
T^i_AIR	air temperature (K)
T_CAT	catalyst temperature (K)
T_dp	gas temperature (dense phase) (K)
T^i_dp	initial gas temperature (dense phase) (K)
T_fb	gas temperature (dilute phase) (K)
T_G	gas temperature (K)
T_p	temperatura de la superficie catalítica en el riser (K)
T^i_VAP	steam temperature (K)
u_fb	gas rate (dilute phase) (m/s)
u_g	gas rate in riser (m/s)
u_p	particle rate (m/s)
u_t	final particle rate (in riser) (m/s)
u_gch	gas rate (dilute phase) (m/s)
W_Cq	total catalyst (dense phase) (Tm)
X_j	feedstock conversion (Adim.)
y_Coke	coke yield (%p)
y_j	mol fraction jth lump (dimensionless)
z	axial coordinate (riser) (m)

Greek symbols

α	catalytic factor (Adim.)
β	$\mathrm{CO/CO_2}$ formation rates ratio on catalytic surface (Adim.)
ε	volumetric void fraction (in riser) ($\mathrm{m^3/m^3}$)
ε_fb	void fraction (in dilute phase of regenerator) ($\mathrm{m^3/m^3}$)
η	empirical composition of hydrogen in coke (Adim.)
κ_p	particle thermal conductivity (W/mk)
μ_g	gas viscosity (in riser) (kg/ms)
ρ_g	gas density (in riser) ($\mathrm{kmol/m^3}$)
ρ_p	catalyst density ($\mathrm{kmol/m^3}$)
$\Re_\mathrm{HNC}$	CO homogeneous oxidation rate ($\mathrm{kmol/m^3\,s}$)
$\Re_\mathrm{HNC}\vert_\mathrm{fb}$	gas combustion rate by homogeneous oxidation in regenerator (dilute phase) ($\mathrm{kmol/m^3\,s}$)
$\Re_j$	reaction rate of "j" lump in riser ($\mathrm{kmol/m^3\,s}$)
σ	$\mathrm{SO_2/SO_3}$ formation rates ratio on catalytic surface ($[\mathrm{kmol/m^3}]^{0.5}$)
Φ	activity factor (dimensionless)

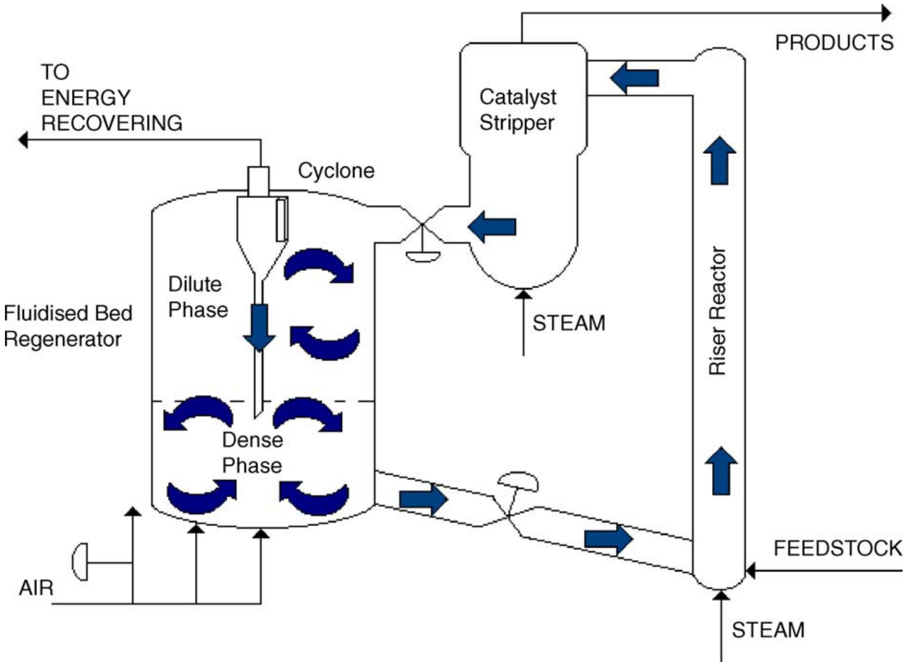

Fig. 1. Typical FCC unit; arrows show catalyst movement.

crude oils, sulphur compounds are more abundant (Table 1). In contrast, sulphur permissible levels in gasoline are becoming smaller each year. Typical FCC gasoline contains mercaptans, thiophenes, substituted thiophenes, thiophenols, tetrahydrothiophene and benzothiophenes [1]. All these compounds are, clearly, undesirable.

The same is true for sulphur oxides emissions allowed in combustion flue gases. SO_x emissions from FCC units have been under standards regulations since 20 years ago. By January 1, 1985, they were reduced below 60 kg/1000 bbl. These regulations limit emissions from a revamped FCC unit to approximately 300 vppm. Regulations are more stringent for new units [1].

Of the total amount of sulphur carried to the regenerator by the spent catalyst, the amount that is emitted as SO_x in the flue gas depends on regenerator operation. Emissions are lower for high regenerator temperatures, low coke on regenerated catalyst (ω_{CRC}), high oxygen excess, high total pressure, and full combustion operating mode [2]. The second, third and fourth factors are antagonistic with respect to the FCC profitability. Therefore it is necessary to find operating regions that fulfil a compromise between minimum impact of the feedstock sulphur on fuels and emissions and good economic operation.

In the following sections, the sulphur cycle in an industrial FCC unit is described and a mathematical model is developed. Numerical solutions of this model are used to characterise the operating region and to find feasible operating points. The main characteristics of the industrial unit used as case study are listed in Table 2.

As it is usual in industrial operation, riser outlet temperature (sometimes called reaction temperature) is the control variable, it means that it is maintained at its set point value. Changes in "catalyst to oil" ratio and airflow rate affect the regenerator operating temperature. In full combustion units, regenerator temperature is not a control variable, because it depends on the coke-burning rate. So the oxygen concentration at the regenerator outlet is controlled by the airflow rate, meanwhile the regenerator temperature establishes [3]. This approach was followed during the simulation of this industrial unit.

1.1. Sulphur in fuels

The main objective of the catalytic cracking process is to obtain valuable fuels, such as gasoline and C_3–C_4 olefins,

Table 1
Typical sulphur compounds in three industrial FCC feed stocks [1]

	VGO Maya	Light Arabic	Gulf blend
Total sulphur (wt.%)	2.77	0.30	2.59
Sulphur compounds composition (wt.%)			
Mercaptans and sulphides	7	12	26
Thiophenes	59	56	42
Benzo and multiring thiophenes	30	17	29
Oxidic sulphur	4	15	3

Table 2
Industrial FCC unit studied

Type	Adiabatic
Operating mode	Full combustion
Feedstock capacity, BPD (kg/s)	25000 (40)
Air-flow rate, average (m^3/h)	75000
Sulphur in feedstock, average (wt.%)	2.30

from a heavy feedstock. Due to the inherent desulphurisation during cracking reactions, which is a consequence of the partial cracking of the C–S bonds in feedstock heterocompounds, sulphur distributes, mainly, to cyclic oils, gasoline, hydrogen sulphide and coke [4]. Higher yield to sour gas is preferable because it implies lower sulphur content in gasoline and coke; also, this by-product is able to be recovered and processed downstream (in Claus and SuperClaus units [4], for example) in order to obtain solid sulphur as value product instead of being emitted sulphur to the environment. In order to take into account the amount of sulphur in these products, a seven lump kinetic scheme [5] and empirical correlations were developed (Appendix A). The objective is to comply with desired sulphur levels in fuels, for example the average sulphur levels in the gasoline pool.

The riser model considers plug-flow of catalyst and hydrocarbon mixture. Classical mass and energy balances were developed for each phase and for each one of the compounds that form the vapour phase. A fourth order Runge-Kutta method was used to integrate the resulting equations in discrete intervals. In each one of these intervals density, velocity, kinetic factors and heat and mass transfer coefficients are updated, on the basis of 33 industrial operating data (proprietary).

1.2. Sulphur in regenerator flue gases

Coke is a solid product that will remain adsorbed to the active surface of the catalyst until it is burned inside the regenerator (see Fig. 1). Because of its contribution to the energy balance, production and combustion rates of coke are two of the most important operating variables inside FCC units. That is the reason to study both reactors coupled instead of each one alone.

The coke consists of carbon and hydrogen, mainly, and may be polluted by sulphur, nitrogen or metals from feedstock. For the goals of this work, an empirical formulae for the coke [6,7] was modified in order to take into account the sulphur content after riser reactions: $CH_\nu S_\sigma$. Combustion of coke follows the kinetic path shown in Eq. (1).

$$\begin{aligned} &CH_\nu S_\sigma + \left[\frac{\eta+2}{2(\eta+1)} + \frac{\nu}{4} + \frac{2\sigma+3}{2(\sigma+1)}\right] O_2 \\ &\quad \rightarrow \frac{\eta}{\eta+1} CO + \frac{1}{\eta+1} CO_2 + \frac{\nu}{2} H_2O \\ &\qquad + \frac{\sigma}{\sigma+1} SO_2 + \frac{1}{\sigma+1} SO_3 \qquad (1) \end{aligned}$$

Here, ν and σ represent the empirical formulae of the coke and η is the relationship between CO and CO_2 formation rates evaluated at the catalyst surface [6,7]. It should be noted that sulphur in coke is able to form sulphur oxides that are emitted as flue gases.

The mathematical model for the regenerator consists of classical mass and energy balances for two physical regions present in fluidised beds: dense phase and freeboard [6]. The dense phase is considered as a dynamic continuous stirred tank reactor and the freeboard as a stationary plug flow reactor. The mathematical model is solved using a fourth order Runge-Kutta method. Kinetic parameters were estimated using 33 industrial operating points (proprietary), and the solution of the model was performed inside the operating region delimited by these points; no extrapolations were made.

Numerical simulations were performed solving simultaneously the coupled models for riser and regenerator. Typical manipulate variables (air flow-rate supplied to the regenerator and mass catalyst to oil ratio) were changed in order to simulate the whole operating zone. Sulphur from feedstock was followed up to sulphur content of fuels, hydrogen sulphide production and sulphur emissions from the regenerator. In all cases, simulated results are presented as lines and industrial data as marks. It is important to note that catalyst properties and additives are not taken into account, explicitly.

2. Results and discussion

The first part of the simulation of the unit was dedicated to find an operating region that complies with requirements of gasoline production, and therefore profitability. This search was performed inside the industrial operating region, in order to propose a feasible set of operating conditions. Results are referred to the catalyst to oil ratio, the most common manipulate variable during FCC operation. Airflow rate supplied to regenerator is used as second parameter; during operation this variable controls the rate of coke combustion and, consequently, energy balance. Airflow rate was varied between 14 and 20 m^3/s during the simulations. In this industrial range, the yield to gasoline reaches its higher level (about 50 wt.%) at cat-to-oil ratios between 9.5 and 10.5 (Fig. 2); these values are in agreement with industrial results. Meanwhile, sulphur in gasoline decreases inversely proportional to catalyst to oil ratio in the same domain (Fig. 3); however this variable minimises at the highest catalyst to oil ratios. Therefore, from

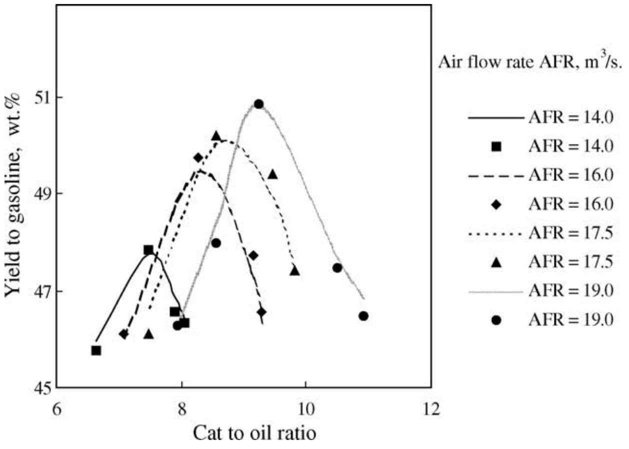

Fig. 2. Yield to gasoline in the operating region studied. Simulated results in lines, industrial data in marks.

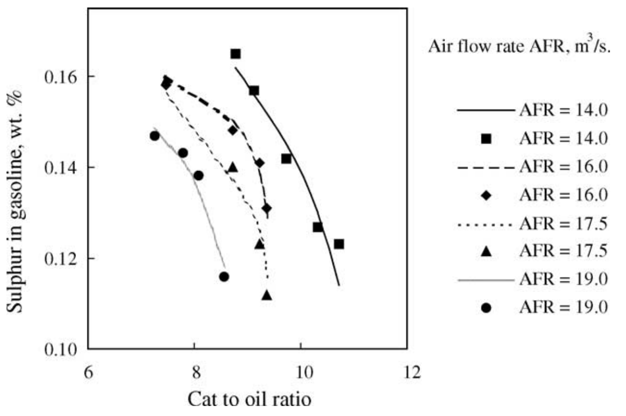

Fig. 3. Sulphur content of gasoline in the operating region studied. Simulated results in lines, industrial data in marks.

the points of view of clean fuels and good profitability, this operating region seems to be very favourable, and in order to evaluate its environmental feasibility emissions have to be analysed too. It is important to note that it is possible to decrease the sulphur content in gasoline by increasing the reaction temperature, which provokes the partial cracking of sulphur compounds in the gasoline [8]; however this operating mode is not considered in this case because the main objective of this FCC unit is to produce the maximum feasible amount of gasoline.

Following the sulphur balance inside the FCC unit, it is possible to see that sour gas production is proportional to the catalyst to oil ratio (Fig. 4). This result is also favourable, because operating at best catalyst to oil values respective to gasoline yields is also an advantage from the environmental point of view. As it was pointed out, higher sour gas yield is preferable instead of sulphur oxides emissions to the environment.

The yield to coke increases proportional to the catalyst to oil ratio in the operating region simulated (Fig. 5). Because this coke is burned at the regenerator, its amount is important in two aspects. Firstly, it controls regenerator temperature and, secondly, some of the sulphur in the coke is able to oxidise. For catalyst to oil ratios between 9 and 10 the amount of coke produced is high, however for higher airflow rates this situation will not be a problem. The following point to look at is the sulphur content of this produced coke.

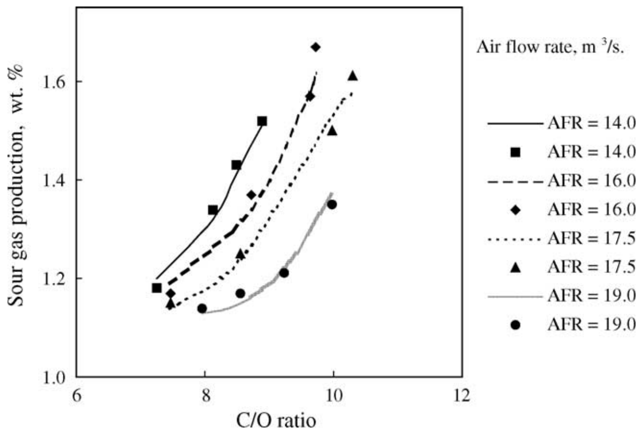

Fig. 4. Sour gas production in the riser. Simulated results in lines, industrial data in marks.

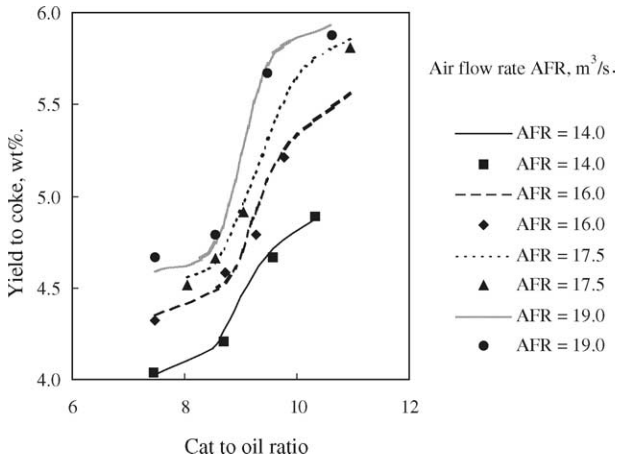

Fig. 5. Yield to coke in the operating region studied. Simulated results in lines, industrial data in marks.

Fortunately, sulphur content in coke decreases inversely proportional to the catalyst to oil rate in this operating region (Fig. 6). For the operating conditions that favour gasoline production, sulphur in coke exhibits values between 1.7 and 2.3 wt.%. Results of sulphur content in gasoline and coke are in agreement with previous studies [1,5].

Sulphur oxides emissions from regenerator are directly proportional to the coke amount and its sulphur content. These emissions decrease inversely proportional to catalyst to oil ratio from 7 to 10, moreover, the curve exhibits its minimum close to a catalyst to oil ratio of 9.5. In contrast, for higher catalyst to oil rates, this trend reverses (Fig. 7). This inversion in the trend is due to the high amount of coke that is burned; even when the relative sulphur level is small, the higher amount of total sulphur in the coke increases the sulphur oxides emissions.

Accordingly to previous results, in order to obtain gasoline with lower content of sulphur and lower emissions of

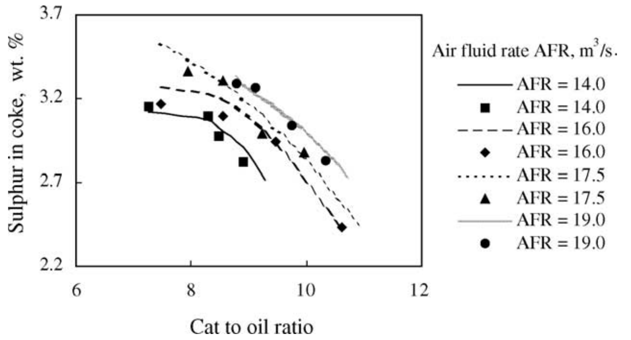

Fig. 6. Sulphur content of coke in the operating region studied. Simulated results in lines, industrial data in marks.

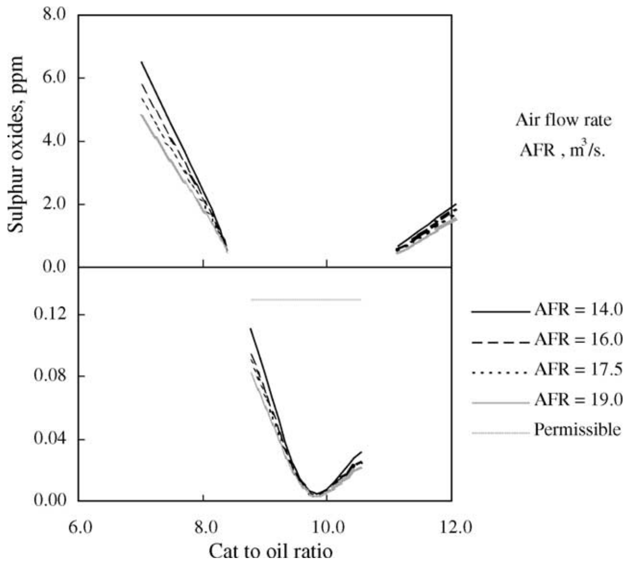

Fig. 7. Sulphur oxide emissions in the operating region studied. Simulated results in lines, industrial data in marks.

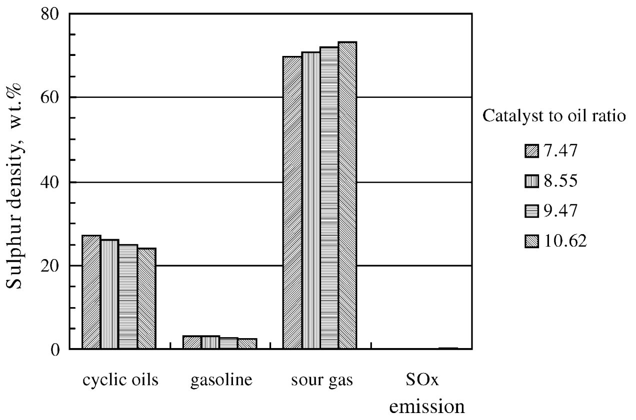

Fig. 8. Distribution of feedstock sulphur among products and emissions. Simulated results.

sulphur oxides, the unit has to be operated at catalyst to oil ratios between 9 and 10. Evaluating the sulphur balance from feedstock to fuels and emissions, it is possible to note that this pollutant is recovered mainly as sour gas; however emissions coming from coke combustion become important at higher catalyst to oil ratios (Fig. 8). This situation provokes a compromise between cleaner gasoline (obtained at higher catalyst to oil ratios) and lower emissions (obtained at intermediate catalyst to oil ratios). In order to perform this sulphur balance, it is necessary to model the FCC unit considering riser and regenerator as a coupled system.

3. Conclusions

A seven-lump kinetic scheme, which specifies the generation of sour gas during catalytic cracking was integrated to a riser mathematical model for an industrial FCC riser. Meanwhile, a comprehensive model for the FCC regenerator, which considers oxidation of sulphur in coke, was coupled to the riser model. Both models were tuned using industrial operating data. Prediction of sour gas formation, sulphur content in final products as well as sulphur distribution in regenerator emissions was performed following a sulphur balance. This model was a helpful tool for modelling steady state FCC operation, taking into account valuable clean fuels production and satisfactory accomplishment of environmental constrains.

It was possible to obtain the best yields to gasoline with lower sulphur content operating at middle catalyst to oil values, close to the industrial ones. In addition, sulphur oxides emissions could be maintained below permissible levels for this operating region. These results should be considered as constrains in order to comply with environmental legislation and economic benefits associated.

Acknowledgements

Authors greatly appreciate the economic support given by the Research Project FIES 98-111-II from the Programa de Tratamiento de Crudo Maya at the Instituto Mexicano del Petróleo. E.F. Villafuerte-Macías thanks CONACYT for the Ph.D. credit-scholarship number 157615.

Appendix A

The following kinetic scheme, which considers the hydrogen sulphide formation [5], is used in this work: typical feedstock (bp 343–565 °C) is cracked into cyclic oils (acs, bp 222–342 °C), gasoline (gsn, bp 35–221 °C), liquid petroleum gas (lpg, C_3–C_4), dry gas (gs, H_2, C_1–C_2), sour gas (H_2S) and solid coke (Table A1). Simultaneously, cyclic oils, gasoline and LPG are able to crack to lighter entities or to form

Table A1
Kinetic parameters used in the model [5]

Cracking reaction	k_0	E (kJ/mol)
Feedstock → cycle oils	240.0	70.0
Feedstock → gasoline	380.0	70.0
Feedstock → LPG	70.5	70.0
Feedstock → dry gas	217.5	80.0
Feedstock → sour gas	2400.0	70.0
Feedstock → coke	0.40	50.0
Cycle oils → gasoline	24.0	60.0
Cycle oils → LPG	30.0	60.0
Cycle oils → dry gas	217.5	60.0
Cycle oils → sour gas	600.0	70.0
Cycle oils → coke	0.60	50.0
Gasoline → LPG	1.0	50.0
Gasoline → dry gas	145.0	70.0
Gasoline → sour gas	300.0	70.0
Gasoline → coke	0.50	50.0
LPG → dry gas	261.0	40.0
LPG → coke	0.40	40.0
Dry gas → coke	1.30	40.0

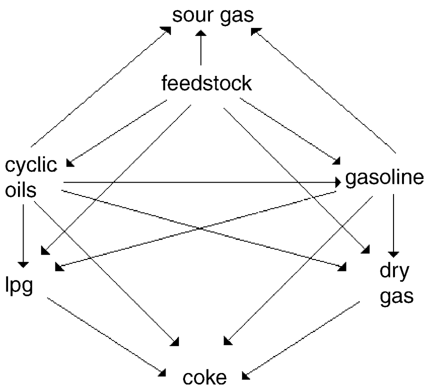

Fig. A.1. Kinetic scheme of the catalytic cracking [5].

solid coke; dry gas is also able to generate coke (Fig. A.1). Coke will remain adsorbed to the catalyst surface until its combustion, situation that will decrease the catalytic activity. A function for the activity after coke deposition, called deactivation function, has been considered [5].

Equations utilised in the simulation of the FCC riser–regenerator system are presented in this appendix. Each equation appears with its corresponding definition as headline.

A.1. Riser reactor

Mass balance for the reacting compound (A) on the catalytic surface:

$$u_{\rm p}\frac{{\rm d}C_{\rm A(p)}}{{\rm d}z} - k_{\rm g}a_{\rm v}\left(\frac{\varepsilon}{1-\varepsilon}C_{\rm A(G)} - C_{\rm A(p)}\right) = \Phi R_j \qquad \text{(A.1)}$$

$$I.C \quad C_{\rm A(p)}(z=0) = C^0_{\rm A(p)} \qquad \text{(A.1.1)}$$

Energy balance for the reacting mixture on the catalyst surface:

$$u_{\rm g}\frac{{\rm d}T_{\rm G}}{{\rm d}z} + \frac{h_{\rm g}a_{\rm v}}{\rho_{\rm g}C_{p({\rm p})}}(T_{\rm G} - T_{\rm p}) = \Phi\sum\frac{(-\Delta H_{\rm r})_j R_j}{C_{p'({\rm p})}} \qquad \text{(A.2)}$$

$$I.C. \quad T_{\rm p}(z=0)T^0_{\rm p} \qquad \text{(A.2.1)}$$

Catalyst deactivation factor (Φ):

$$\Phi = \frac{1}{1+\alpha y_{\rm coke}} \qquad \text{(A.3)}$$

Mass transfer coefficient:

$$k_{\rm G} = 0.57\left(\frac{G_{\rm g}}{\rho_{\rm g}}\right){\rm Re}^{-0.41}{\rm Sc}^{-2/3} \qquad \text{(A.4)}$$

Heat transfer coefficient:

$$h_{\rm g} = 0.6\frac{\kappa_{\rm p}}{d_{\rm p}}{\rm Pr}\times{\rm Re}^{0.3} \qquad \text{(A.5)}$$

Reaction rates for cracking of feedstock to products:

$$R_{\rm feedstock} = -\sum_j k_{{\rm feedstock}-j}\exp(-E_{{\rm feedstock}-j}/R_{\rm g}T)C^2_{\rm feedstock},$$

$$j = \text{acs, gsn, LPG, gs, H}_2\text{S, coke} \qquad \text{(A.6)}$$

Similar reaction rate expressions are used for the cracking of lighter products:

$$R_{\rm lump} = -\sum_j k_{{\rm llump}-j}\exp(-E_{{\rm lump}-j}/R_{\rm g}T)C_{\rm lump},$$

$$j = \text{gsn, LPG, gs, H}_2\text{S, coke} \qquad \text{(A.7)}$$

Sulphur content of products (cycle oils, gasoline and coke) is calculated applying empirical functions. Such functions depend on feedstock volume conversion [4].

$$S_{\rm LC} = (a + bX + cX^2) \qquad \text{(A.8)}$$

Numerical values of a, b, c depend on feedstock and cracking product. They are calculated by using statistical techniques, and adjusted according to industrial results. These empirical models calculate the weight percent of sulphur content in cyclic oils, gasoline and coke.

Kinetic and empiric parameters for sulphur distribution were fitted by using 33 industrial operating points (proprietary), some of them with different operating conditions. During the simulation of the industrial unit, the operating region was chosen inside the industrial operating region and no extrapolations were made.

A.2. Regenerator reactor

Mass balance in dense phase for O_2, CO, CO_2 and SO_x:

$$\frac{{\rm d}N_{\rm O_2dp}}{{\rm d}t} = G^i_{\rm O_2} - G_{\rm O_2} + R_{\rm O_2}|_{\rm dp} \qquad \text{(A.9)}$$

$$\frac{{\rm d}N_{\rm COdp}}{{\rm d}t} = G^i_{\rm CO} - G_{\rm CO} + R_{\rm CO}|_{\rm dp} \qquad \text{(A.10)}$$

$$\frac{{\rm d}N_{\rm CO_2dp}}{{\rm d}t} = G^i_{\rm CO_2} - G_{\rm CO_2} + R_{\rm CO_2}|_{\rm dp} \qquad \text{(A.11)}$$

$$\frac{{\rm d}N_{{\rm SO}_x{\rm dp}}}{{\rm d}t} = G^i_{{\rm SO}_x} - G_{{\rm SO}_x} + R_{{\rm SO}_x}|_{\rm dp} \qquad \text{(A.12)}$$

$R_{\rm O_2}$, $R_{\rm co}$, $R_{\rm CO_2}$ and $R_{{\rm SO}_x}$ depend on catalyst weight, stoichiometric coefficient and rate reaction of coke combustion. For example in the case of sulphur oxides:

$$R_{{\rm SO}_x}|_{\rm dp} = W_{\rm Cq}\nu_{{\rm SO}_x}\mathfrak{R}_{\rm Cq} \qquad \text{(A.13)}$$

Mass balance in dilute phase for O_2, CO, CO_2 and SO_x:

$$\left.\frac{{\rm d}G_{\rm O_2}}{{\rm d}z_{\rm fb}}\right|_{\rm fb} = \frac{R_{\rm O_2}|_{\rm fb}}{u_{\rm gch}} \qquad \text{(A.14)}$$

$$\left.\frac{{\rm d}G_{\rm CO}}{{\rm d}z_{\rm fb}}\right|_{\rm fb} = \frac{R_{\rm CO}|_{\rm fb}}{u_{\rm gch}} \qquad \text{(A.15)}$$

$$\left.\frac{\mathrm{d}G_{\mathrm{CO_2}}}{\mathrm{d}z_{\mathrm{fb}}}\right|_{\mathrm{fb}} = \frac{R_{\mathrm{CO_2}}|_{\mathrm{fb}}}{u_{\mathrm{gch}}} \qquad \text{(A.16)}$$

$$\left.\frac{\mathrm{d}G_{\mathrm{SO}_x}}{\mathrm{d}z_{\mathrm{fb}}}\right|_{\mathrm{fb}} = \frac{R_{\mathrm{SO}_x}|_{\mathrm{fb}}}{u_{\mathrm{gch}}} \qquad \text{(A.17)}$$

$R_{\mathrm{O_2}}$, R_{CO},$R_{\mathrm{CO_2}}$and R_{SO_x}depend on stoichiometric coefficient and rate reaction of coke, CO and $\mathrm{CO_2}$ combustion.

Energy balance for the dense phase:

$$\begin{aligned}\frac{\mathrm{d}T_{\mathrm{dp}}}{\mathrm{d}t} &= \frac{(G^{i}_{\mathrm{O_2}} + G^{i}_{\mathrm{N_2}})C^{i}_{p\mathrm{AIR}}T^{i}_{\mathrm{AIR}}}{W_{\mathrm{Cq}}C_p} \\ &+ \frac{(G_{\mathrm{O_2}} + G_{\mathrm{CO}} + G_{\mathrm{CO_2}} + G_{\mathrm{H_2O}} + G_{\mathrm{SO_2}} + G^{i}_{\mathrm{N_2}})C_p T_{\mathrm{dp}}}{W_{\mathrm{Cq}}C_p} \\ &+ \frac{G^{i}_{\mathrm{VAP}}C_p(T^{i}_{\mathrm{VAP}} - T_{\mathrm{dp}}) + (m^{i}_{\mathrm{CAT}}T^{i}_{\mathrm{CAT}} - m_{\mathrm{CAT}}T_{\mathrm{dp}})C_p + \sum_{j=1}^{j=5}(-\Delta H_j)\Re_j|_{\mathrm{dp}}}{W_{\mathrm{Cq}}C_p} \qquad \text{(A.18)}\end{aligned}$$

Energy balance for the dilute phase:

$$\frac{\mathrm{d}T_{\mathrm{fb}}}{\mathrm{d}z} = \frac{(-\Delta H)_{\mathrm{HNC}}\Re_{\mathrm{HNC}}|_{\mathrm{fb}}}{(1-\varepsilon_{\mathrm{fb}})\rho_{\mathrm{p}}C_p + \varepsilon_{\mathrm{fb}}C_p\left(\sum y_j PM_j\right)u_{\mathrm{gch}}} \qquad \text{(A.19)}$$

Dimensionless numbers

$$\mathrm{Nu} = \frac{h_{\mathrm{g}}d_{\mathrm{p}}}{k_{(\mathrm{g})}} \qquad \text{(in riser)} \qquad \text{(A.20)}$$

$$\mathrm{Pr} = \frac{C_{p(\mathrm{G})}\mu_{\mathrm{g}}}{k_{(\mathrm{g})}} \qquad \text{(in riser)} \qquad \text{(A.21)}$$

$$\mathrm{Re} = \frac{d_{\mathrm{p}}u_{\mathrm{t}}\rho_{\mathrm{g}}}{\mu_{\mathrm{g}}} \qquad \text{(in riser)} \qquad \text{(A.22)}$$

$$\mathrm{Re} = \frac{G_{\mathrm{g}}}{a_{\mathrm{v}}\phi\mu_{\mathrm{g}}} \qquad \text{(In regenerator)} \qquad \text{(A.23)}$$

$$\mathrm{Sc} = \frac{\mu_{\mathrm{g}}}{\rho_{\mathrm{g}}D_{\mathrm{V}}} \qquad \text{(in regenerator)} \qquad \text{(A.24)}$$

References

[1] W.C. Cheng, G. Kim, A.W. Peters, X. Xhao, K. Rajagopalan, M.S. Ziebarth, C.J. Pereira, Environmental fluid catalytic cracking technology, Cat. Rev., Sci. Eng. 40 (1998) 39–79.

[2] D.P. Mc Arthur, H.D. Simpson, K. Baron, Catalytic control of FCC SOX emissions looking good, Oil Gas J. 23 (1981) 55–59.

[3] A.A. Arbel, I.H. Rinard, R. Shinnar, Dynamics and control of fluidized catalytic crackers. 3. Designing the control system: choice of manipulated and measured variables for partial control, IECh Res. 35 (1996) 2215–2233.

[4] P.B. Venuto, E.T. Habib, Catalyst-feedstock-engineering interactions in fluid catalytic cracking, Catal. Rev., Sci. Eng. 18 (1978) 1–150.

[5] E.F. Villafuerte-Macías, Ricardo Aguilar, R. Maya-Yescas, Towards modelling production of clean fuels: sour gas formation in catalytic cracking, J. Chem. Tech. Biotechnol. 79 (2004) 1113–1118.

[6] A.F. Errazu, H.I. de Lasa, F. Sarti, A fluidized bed catalytic cracking regenerator model: grid effects, Can. J. Chem. Eng. 37 (1979) 191–197.

[7] A. Krishna, E. Parkin, Modeling the regenerator in commercial fluid catalytic cracking units, Chem. Eng. Prog. (1985) 57–61.

[8] A. Corma, C. Martínez, G. Ketley, G. Blair, On the mechanism of sulphur removal during catalyst cracking, Appl. Catal. A: Gen. 208 (2001) 135–152.